Intelligence & Control
https://www.sciltp.com/journals/ic

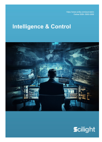

Article

Fast Finite-Time Adaptive Consensus with Prescribed Performance Tracking Control for High-Power Nonlinear MASs

Xiao Zheng [1], Yuanzhao Chen [1], Xiaomei Wang [2,*], Xiaoqing Zhang [1] and Yi Niu [1,*]

[1] The School of Information Science and Engineering, Shandong Normal University, Jinan 250014, China
[2] The School of Automation, Chongqing University, Chongqing 400044, China
* Correspondence: wlwxmei@163.com (X.W.); niuyi@sdnu.edu.cn (Y.N.)

How To Cite: Zheng, X.; Chen, Y.; Wang, X; et al. Fast Finite-Time Adaptive Consensus with Prescribed Performance Tracking Control for High-Power Nonlinear MASs. *Intelligence & Control* **2025**, *1*(1), 4. https://doi.org/10.53941/ic.2025.100004

Received: 23 July 2025
Revised: 19 August 2025
Accepted: 1 September 2025
Published: 17 September 2025

Abstract: This paper addresses the challenge of achieving fast finite-time adaptive consensus tracking control and prescribed performance control for a category of high-power uncertain nonlinear multi-agent systems (MASs) under external signal disturbances. First, a new error coordinate transformation scheme is devised to effectively decouple local and neighbor information. Second, by ensuring that all signals in the closed-loop system remain bounded, the controller is equipped with sufficient capability to compensate for the system's unknowns, external disturbance signals, and parameter uncertainties, thereby achieving consensus tracking performance. In comparison to traditional tracking control strategies, the proposed control method guarantees that the output of the MASs asymptotically converges to zero. Third, to meet the performance requirements of MASs, a prescribed performance function is designed to constrain the errors in the finite-time control framework, thereby enhancing both the transient and steady-state performance of the system. The proposed control mechanism guarantees that the MASs meet the performance requirements within a finite time. Finally, simulation results demonstrate the effectiveness of the proposed control mechanism.

Keywords: adaptive consensus tracking control; nonlinear high-power multi-agent systems; prescribed performance; fast finite-time stabilization; power integration technique

1. Introduction

With the advancements of multi-agent systems (MASs), agents need to collaborate efficiently in various application scenarios to complete complex tasks. Through communication and cooperation among agents, MASs can achieve distributed control and decision-making in intricate environments, such as drone swarms, robotic groups, and intelligent transportation systems [1–3]. As computing power and communication technology develop continuously, research in MASs has significantly progressed, particularly in the control methods for linear MASs.

These methods mainly focus on consensus control, swarm collaboration, and task allocation [4–6]. Nonetheless, the assumption of linear systems restricts their ability to effectively address the nonlinear characteristics common in many systems. In particular, when facing dynamic changes and complex environments, linear models frequently fail to accurately describe system behavior, thereby limiting system performance. To overcome the limitations of linear systems, nonlinear MASs have emerged as a research hotspot. Nonlinear systems can more accurately express complex dynamic behaviors, and studies indicate that nonlinear control methods can complete consensus and tracking tasks in more complex environments, providing enhanced robustness and adaptability [7]. Compared to linear systems, nonlinear MASs are capable of addressing more complex issues, such as dynamic uncertainties and external disturbances. Within the realm of nonlinear systems, high-power nonlinear systems present particularly significant challenges. Their dynamic models typically incorporate complex nonlinear terms, complicating stability

Copyright: © 2025 by the authors. This is an open access article under the terms and conditions of the Creative Commons Attribution (CC BY) license (https://creativecommons.org/licenses/by/4.0/).
Publisher's Note: Scilight stays neutral with regard to jurisdictional claims in published maps and institutional affiliations.

analysis and control design [8]. The control of high-power nonlinear systems should not only ensure system stability but also guarantee efficient collaboration and consensus among agents. Though existing studies have investigated control methods for high-power nonlinear systems, most assume that the system operates in an ideal environment, failing to fully consider external disturbances and system uncertainties [9]. Nonetheless, in practical applications, disturbances and uncertainties are inevitable, with factors such as environmental changes, sensor errors, and actuator noise all impacting system performance. Consequently, achieving consensus and efficient control in uncertain and disturbed environments has become a pressing challenge [10]. Moreover, existing studies have not thoroughly addressed the issue of gain design, which is crucial for system performance, as appropriate gain selection can significantly affect system response speed, stability, and robustness to disturbances [11]. In high-power nonlinear MASs, how to adjust the gain based on the system's dynamic characteristics to ensure system stability and efficient performance remains an urgent problem.

In the field of multi-agent systems, Finite-Time Control (FTC) is emerging as an important control method. Unlike traditional asymptotic stability control [12], Fast FTC can drive the system state to the target state within a specified finite time, providing significant advantages, particularly in the face of uncertainty and nonlinear challenges. Traditional methods may struggle to guarantee stability and performance in high-power uncertain nonlinear systems due to system complexity, while fast FTC offers an effective solution [13]. The key feature of FTC lies in designing control laws that ensure the system state converges to the target value within the specified time, exhibiting strong robustness, which makes it particularly outstanding in MASs. Studies have indicated that fast FTC can achieve consensus objectives and maintain system stability within a finite time. For instance, Shang et al. proposed an adaptive FTC method for uncertain nonlinear systems that achieves consensus tracking in finite time [14]; Zou et al. resolved the finite-time consensus problem in MASs and introduced a new protocol to ensure consensus in finite time, even under uncertainty [15]. In addition, Lei et al. developed an adaptive FTC method for highly uncertain nonlinear systems, ensuring precise coordination among multi-agents in finite time [16]. Although FTC has demonstrated considerable potential in MASs, designing effective control strategies in high-power uncertain nonlinear systems remains a challenge. In recent years, researchers have integrated adaptive control with FTC to devise new methods to address dynamic changes and uncertainties in the system. These methods automatically adjust control parameters to enhance system stability and tracking performance within the specified time. Therefore, FTC provides an effective control mechanism for high-power uncertain nonlinear MASs, ensuring system stability while achieving consensus tracking tasks within a finite time.

Prescribed Performance Control (PPC) is a method for designing controllers by establishing performance requirements. Distinguished from traditional stability control, PPC emphasizes not only stability but also performance indicators such as steady-state error, response speed, and control energy. PPC has demonstrated significant application value in MASs and complex network control, especially in high-power uncertain nonlinear systems [17], where the key challenge lies in meeting performance objectives while ensuring stability. Given the complex dynamic behavior and uncertainties in MASs, designing control strategies becomes increasingly challenging. To address this issue, researchers have developed various PPC-based control methods. For instance, an adaptive control mechanism devised in [18] achieves consistency and performance requirements under system uncertainties and disturbances. Sui et al. proposed a PPC method that incorporates nonlinear system characteristics, enhancing stability and response speed by optimizing performance indicators [19]. Furthermore, combining PPC with FTC further improves system performance. As a rapid convergence method, FTC is particularly suitable for MASs requiring fast response. By integrating PPC, the system can achieve predefined performance objectives within a finite time while reducing control inputs and minimizing energy consumption. The finite-time PPC method proposed in [20] significantly improves dynamic response and stability under uncertainty. PPC provides a flexible and efficient control solution for MASs, ensuring stability and achieving performance objectives even under uncertainty and nonlinear characteristics. When integrated with FTC, it enables precise control in a short time, making it particularly suitable for high-precision and rapid response scenarios.

Inspired by the above discussion, this paper proposes a new adaptive consensus tracking control for high-power nonlinear MASs based on the adaptive compensation technique. Compared to existing works, our work has the following advantages:

(i) This paper proposes a control mechanism based on prescribed performance aimed at enhancing the tracking accuracy and robustness of MASs under uncertainty and nonlinearity. By prescribing the system performance, the controller can predefine the desired dynamic behavior, thus ensuring system stability and reliability. In contrast to [17,18,20], this approach effectively addresses the uncertainty issue in performance estimation inherent in traditional methods.

(ii) This paper introduces a fast FTC method to tackle the consensus tracking problem in high-power uncertain nonlinear MASs. By utilizing an adaptive controller, the system can achieve consensus within a finite time while effectively managing uncertainty and nonlinearity. Compared to traditional asymptotic stability control methods, including [21–23], FTC significantly enhances the system's response speed and convergence, meets stringent time performance requirements, and effectively reduces tracking errors, thereby improving overall system performance.

(iii) This paper proposes an adaptive consensus control mechanism that adjusts the controller parameters in real-time to address the challenges posed by dynamic environments and uncertainties in MASs. The mechanism employs an adaptive algorithm to adjust the gain parameters online, ensuring that all agents achieve consensus tracking within a finite time, even when system parameters are not fully known. Compared to approaches discussed in [24–26], this method enhances system adaptability and ensures robustness and stability in uncertain and nonlinear environments.

2. Preliminaries and Problem Establishment

2.1. Basic Graph Theory

The directed graph can be denoted as $G = (U, N_L)$, where $U = \{u_1, ..., u_k\}$ denotes the node set and $N_L \subseteq U \times U$ represents the edge set. $e_{ji} = (u_j, u_i) \in N_L$ represents the edge, indicating that the agent i can receive information from agent j. In the directed graph, the adjacency matrix can be denoted as $A = [a_{ij}] \in R^{k\times k}$, where if $e_{ji} = (u_j, u_i) \in N_L$, then $a_{ij} > 0$. The case of self-loops is usually not considered. Let $D = \text{diag}(d_1, ..., d_k) \in R^{k\times k}$ be the in-degree matrix where $d_i = \sum_{j=1}^{N} a_{ij}$. Then, the Laplacian matrix can be denoted as $L = D - A$ in the directed graph G. Additionally, a matrix $B = \text{diag}(b_1, ..., b_k) \in R^{k\times k}$ is defined, where b_k denotes the weight between the leader and agent k.

When considering the leader, an augmented graph $\bar{G}$ is typically utilized to represent the communication topology between the leader and the followers. $\bar{G} = (\bar{V}, \bar{E})$ is an augmented graph based on the aforementioned graph G, where $\bar{V}$ and $\bar{E}$ denote the corresponding node set and edge set of $\bar{G}$, respectively. $\bar{V}$ contains the leader and followers, and $\bar{E}$ indicates the information flow among the leader and the followers.

2.2. Problem Establishment

This paper considers nonlinear MASs, which typically consist of N ($N \geq 2$) followers (labeled 1 to N) and a leader (labeled r). The communication topology of the followers is described by a graph G. The dynamic model of the i-th ($\forall i \in \{1, 2, ..., N\}$) follower is given by

$$\begin{cases} \dot{x}_{i,k}(t) = g_{i,k}(t, \bar{x}_{i,n})x_{i,k+1}^{p_{i,k}} + f_{i,n}(t, \bar{x}_{i,n}) + d_{i,k}, \\ \dot{x}_{i,n}(t) = g_{i,n}(t, \bar{x}_{i,n})u_i^{p_{i,n}} + f_{i,n}(t, \bar{x}_{i,n}) + d_{i,n}, \\ y_i(t) = x_{i,1}(t), \end{cases} \tag{1}$$

where $k = 1, \ldots, n-1$, $x_{i,1}, ..., x_{i,n} \in R^n$ are the state variables of the i-th agent, $y_i(t) \in \mathbb{R}$ and $u_i \in \mathbb{R}$ respectively represent the output and input of the i-th follower, and $\bar{x}_{i,k} = (x_{i,1}, ..., x_{i,k})$ is the system state vector. The unknown nonlinear functions $f_{i,k}(\bar{x}_{i,k})$ and $g_{i,k}(\bar{x}_{i,k})$ are continuous. The function d_i depicts a continuous time-varying disturbance signal, satisfying $|d_i| \leq \sigma$, where σ is an unknown constant. For brevity, let $x_{i,n+1} = u_i$.

The dynamic of the leader agent is modeled by

$$\begin{aligned} \dot{x}_r &= f_r(x_r, t), \\ y_r &= x_r, \end{aligned} \tag{2}$$

where $y_r \in \mathbb{R}$ represents the output of the leader, and $f_r(x_r, t)$ denotes a piecewise continuous function with respect to time t and satisfying the locally Lipschitz condition with respect to x_r for $t \geq 0$.

Assumption 1. *For any continuously differentiable reference signal $y_r(t)$ and its derivative $\dot{y}_r(t)$, there exists an unknown positive constant M such that $|y_r(t)| + |\dot{y}_r(t)| \leq M$.*

Remark 1. *Distinguished from the existing practical tracking results [27–29], which assume that the tracking signal $y_r(t)$ and its n-th power derivative are known and bounded, this paper only requires that the tracking signal $y_r(t)$ and its first-order derivative are bounded. In addition, the existence of the unknown constant M challenges conventional strategies.*

Assumption 2. *The communication graph is directed and includes a spanning tree rooted at the leader signal y_r, ensuring that at least one follower can directly obtain and utilize all information of the leader signal.*

Assumption 3. *There exists a known smooth positive function $\gamma_{i,k}(\bar{x}_{i,k})$ and an unknown positive constant $c_i > 0$ such that*

$$|f_{i,k}(\bar{x}_{i,k})| \leq c_i \gamma_{i,k}(\bar{x}_{i,k}). \tag{3}$$

Assumption 4. *The sign of $g_i(\bar{x}_i, t)$ is unknown, $i = 1, \ldots, n-1$, but there exist unknown continuous positive functions $\bar{g}_{i,k}$, and $\underline{g}_{i,k}$ such that the following conditions are satisfied:*

$$\underline{g}_i(\bar{x}_i) \leq |g_i(\bar{x}_i)| \leq \bar{g}_i(\bar{x}_i). \tag{4}$$

The following presents several technical lemmas that are crucial in the design process.

Lemma 1 ([30]). *For a given constant $\varepsilon > 0$ and any $x \in \mathbb{R}$, the following holds*

$$0 \leq |x| - \frac{x^2}{\sqrt{x^2 + \varepsilon^2}} < \varepsilon. \tag{5}$$

Lemma 2 ([31]). *Based on Assumption 2, the symmetric positive definite matrix is defined as $Q = (L+B)+(L+B)^T$.*

Lemma 3 ([32]). *For any real-valued continuous function $\Phi(x, y)$ with $x \in \mathbb{R}^m$ and $y \in \mathbb{R}^n$, there exist smooth functions $\Phi_1(x) \geq 0, \Phi_2(y) \geq 0, \Phi_3(x) \geq 1,$ and $\Phi_4(y) \geq 1$ such that $|\Phi(x, y)| \leq \Phi_1(x) + \Phi_2(y)$ and $|\Phi(x, y)| \leq \Phi_3(x)\Phi_4(y)$.*

Lemma 4 ([33]). *For any $x, y \in \mathbb{R}$ and a given constant $p \geq 1$, make $|x \pm y| \leq 2^{1-\frac{1}{p}} \left(|x^p \pm y^p|\right)^{\frac{1}{p}}$.*

Lemma 5 ([34]).

$$\begin{aligned} |a(x, y)x^m y^n| \leq & \frac{n}{m+n} \left(\frac{m}{(m+n)c(x, y)} \right)^{\frac{m}{n}} |a(x, y)|^{\frac{m+n}{n}} \\ & \cdot |y|^{m+n} + c(x, y)|x|^{m+n}, \end{aligned} \tag{6}$$

where $c(x, y) > 0$.

Lemma 6 ([35]). *For a given constant $p > 0$ and any $x_i (i = 1, \ldots, N)$, we have $(|x_1| + \ldots + |x_n|)^p \leq c\left(|x_1|^p + \ldots + |x_n|^p\right)$, where $c = 1$ for $p \in (0, 1)$, and $c = n^{p-1}$ for $p \in [1, \infty)$.*

Lemma 7 ([36]). *Consider a nonlinear system $\dot{z} = \phi(z)$. Let $V(z)$ be a smooth, positive definite function. If there exist some scalars $a > 0$, $b > 0$, $\rho > 0$ and $0 < \gamma < 1$ such that $\dot{V}(z) \leq -aV^\gamma(z) - bV(z) + \rho$, then for a scalar τ with $0 < \tau < b$, there exists a constant $T > 0$ such that for all $t \geq T$, $V(z(t)) \leq \frac{\rho}{b-\tau}$, with T being defined by $T = t_0 + \frac{1}{\tau(1-\gamma)} \ln \left(\frac{\frac{a}{\tau} + V(t_0)^{1-\gamma}}{\frac{a}{\tau} + \left(\frac{\rho}{b-\tau}\right)^{1-\gamma}} \right)$.*

2.3. Finite-Time Prescribed Performance

Definition 1. *A smooth function $\rho(t)$ satisfies the following condition:*

1. $\rho(t) > 0$;
2. $\dot{\rho}(t) \leq 0$;
3. $\lim_{t \to t_r} \rho(t) = \rho_{t_r}$, *and ρ_{t_r} is a positive constant;*
4. *when $t \geq t_r$, $\rho(t) = \rho_{t_r}$ with t_r being a set time.*

Then, $\rho(t)$ is a finite-time performance function [37], and inspired by [38], it can be defined as follows:

$$\rho(t) = \begin{cases} \left(\rho_0^\ell - \ell J t\right)^{\frac{1}{\ell}} + \rho_{tr}, & 0 \leq t < t_r \\ \rho_{tr}, & t \geq t_r \end{cases} \tag{7}$$

where ℓ, J, ρ_{t_r}, and ρ_0^ℓ are positive parameters. Additionally, $\rho_0 + \rho_{t_r} = \rho(0)$ is the initial value, and $t_r = \frac{\rho_0^\ell}{\ell J}$ is the set time.

3. Design Adaptive Controller

In this section, an adaptive consensus tracking controller for high-power nonlinear MASs (1) is devised using backstepping, and coordinate transformations are introduced as follows

$$\begin{cases} m_{i,1}(t) = x_{i,1}(t) - y_r(t), \\ z_{i,1}(t) = \tan(\frac{\pi m_{i,1}(t)}{2\rho(t)}), \\ z_{i,k}(t) = x_{i,k}^{p_{i,1}\cdots p_{i,k-1}}(t) - \alpha_{i,k}^{p_{i,1}\cdots p_{i,k-1}}(\bar{x}_{i-1,k}(t), y_r, \hat{\theta}), \end{cases} \tag{8}$$

where $m(t)$ denotes the tracking error with $y_r(t)$ being the reference signal, $i = 1, 2, ..., N$, $k = 2, \cdots, n-1$; $\alpha_{i,k}^{p_{i,1}\cdots p_{i,k-1}}$ is referred to as the virtual controller, which is defined with respect to $y_r, \bar{x}_{j,k-1}, \bar{x}_{i,k-1}$ and $\hat{\theta}_i$.

Taking the time derivative of $\dot{z}_{i,1}(t)$, we have

$$\dot{z}_{i,1}(t) = \frac{\pi(\dot{m}_{i,1}(t)\rho(t) - m_{i,1}(t)\dot{\rho}(t))}{2\rho^2(t)\cos^2(\frac{\pi m_{i,1}(t)}{2\rho(t)})} = A_i\dot{m}_{i,1}(t) + H_i, \tag{9}$$

where

$$A_i = \frac{\pi}{2\rho\cos^2(\frac{\pi m_{i,1}}{2\rho})}, H_i = -\frac{\pi m_{i,1}\dot{\rho}}{2\rho^2\cos^2(\frac{\pi m_{i,1}}{2\rho})}. \tag{10}$$

Motivated by [39,40], the consensus tracking error for agent i can be expressed as

$$e_i = \sum_{j=1}^{N} a_{ij}(y_i - y_j) + b_i(y_i - y_r), \tag{11}$$

where $i = 1, 2, \ldots, N$, $e = \left[e_1, e_2, \ldots, e_N\right]^T \in \mathbb{R}^N$, and b_i represents the weight between the i-th agent and the leader agent. Define $m = [m_1, m_2, \ldots, m_N]^T$, and then we have $e = (L + B)m$.

Define a function as

$$W_{i,k} = \int_{\alpha_{i,k-1}}^{x_{i,k}} (s^{p_{i,1}\cdots p_{i,k-1}} - \alpha_{i,k-1}^{p_{i,1}\cdots p_{i,k-1}})^{2-\frac{1}{p_{i,1}\cdots p_{i,k-1}}} ds, \tag{12}$$

where $k = 2, ..., n$.

The properties of W_k are described as follows.

Proposition 1 ([34]). *W_k is continuously differentiable and satisfies*

$$\begin{cases} \frac{\partial W_{i,k}}{\partial x_{i,k}} = z_{i,k}^{2-\frac{1}{p_{i,1}\cdots p_{i,k-1}}}, \quad i = 1, \ldots, 2k+1. \\ \frac{\partial W_{i,k}}{\partial \omega_{i,k}} = \varpi_{i,k} \frac{\partial \alpha_{i,k}^{p_{i,1}\cdots p_{i,k-1}}}{\partial \omega_{i,k}}, \end{cases} \tag{13}$$

where $\omega_{i,1} = y_r, \omega_{i,2} = \hat{\theta}_i, \omega_{i,2+j} = x_{i,j} (j = 1, \ldots, k-1)$ and $\varpi_{i,k} = -(2 - \frac{1}{p_{i,1}\cdots p_{i,k-1}}) \int_{\alpha_{i,k-1}}^{x_{i,k}} (s^{p_{i,1}\cdots p_{i,k-1}} - \alpha_{i,k-1}^{p_{i,1}\cdots p_{i,k-1}})^{1-\frac{1}{p_{i,1}\cdots p_{i,k-1}}} ds$. Furthermore, there is a known constant $\Psi > 0$ such that $W_k \geq \Psi(x_{i,k} - \alpha_{i,k-1})^{2p_{i,1},\ldots,p_{i,k-1}}$.

Step 1: In this step, choose the Lyapunov function V_1 as

$$V_1 = \frac{1}{2}z_1^T z_1 + \frac{1}{2}\tilde{\theta}^T\tilde{\theta}, \tag{14}$$

where $z_1 = [z_{1,1}, z_{2,1}, \ldots, z_{N,1}]^T$, and the error vector is $\tilde{\theta} = \theta - \hat{\theta}$ with $\hat{\theta} = [\hat{\theta}_1, \hat{\theta}_2, \ldots, \hat{\theta}_N]$ denoting the estimation of the unknown $\theta = [\theta_1, \theta_2, \ldots, \theta_N]$ and $\theta_i = \max\{c_i, M\}$.

Differentiating V_1 and alone Equation (8) yields

$$\dot{V}_1 = z_1^T(A_i\dot{m}_{i,1}(t) + H_i) - \tilde{\theta}^T\dot{\hat{\theta}}. \tag{15}$$

Then, the time derivative of V_1 along the trajectories of Equation (8) is given by

$$\begin{aligned}\dot{V}_1 =&\sum_{i=1}^{N}\Bigg[-\left(\frac{k_{i,1}z_{i,1}^2}{2}\right)^{\frac{1}{2}}-\frac{c_{i,1}z_{i,1}^2}{2}+\frac{c_{i,1}z_{i,1}^2}{2}+A_iz_{i,1}f_{i,1}\\&+\left(\frac{k_{i,1}z_{i,1}^2}{2}\right)^{\frac{1}{2}}+A_ig_{i,1}z_{i,1}z_{i,2}+A_ig_{i,1}z_{i,1}\alpha_{i,1}^{p_{i,1}}\\&+A_iz_{i,1}d_{i,1}-A_iz_{i,1}\dot{y}_r+H_iz_{i,1}-\tilde{\theta}_i\dot{\hat{\theta}}_i\Bigg],\end{aligned} \tag{16}$$

where $k_{i,1}$ and $c_{i,1}$ are positive design parameters, and this holds true for subsequent cases.

By Assumptions 1 and 3 and Equation (12), we have

$$\begin{aligned}&\left(\frac{k_{i,1}z_{i,1}^2}{2}\right)^{\frac{1}{2}}+A_iz_{i,1}f_{i,1}+A_iz_{i,1}d_{i,1}+H_iz_{i,1}-A_iz_{i,1}\dot{y}_r\\&\leq\theta_i\Bigg(\frac{6A_i^2\gamma_{i,1}^2}{\sqrt{36z_{i,1}^2\gamma_{i,1}^2A_i^2+\varepsilon_{i,1}^2}}+\frac{6A_i^2}{\sqrt{36z_{i,1}^2A_i^2+\varepsilon_{i,1}^2}}\\&\quad+\frac{6k_{i,1}}{\sqrt{36k_{i,1}z_{i,1}^2+\varepsilon_{i,1}^2}}+\frac{6\beta^2A_i^2}{\sqrt{36z_{i,1}^2\beta^2A_i^2+\varepsilon_{i,1}^2}}\\&\quad+\frac{6H_i^2}{\sqrt{36z_{i,1}^2H_i^2+\varepsilon_{i,1}^2}}\Bigg)z_{i,1}^2+\frac{5\theta_i\varepsilon_{i,1}}{6}\\&\triangleq\theta_i\varphi_{i,1}z_{i,1}^2+\frac{5\theta_i\varepsilon_{i,1}}{6},\end{aligned} \tag{17}$$

where $\varepsilon_{i,1}>0$ is an arbitrary constant, and $\varphi_{i,1}$ is a smooth positive function.

Substituting Equation (17) into Equation (16) yields

$$\begin{aligned}\dot{V}_1 \leq&\sum_{i=1}^{N}\Bigg[-\left(\frac{k_{i,1}z_{i,1}^2}{2}\right)^{\frac{1}{2}}-\frac{c_{i,1}z_{i,1}^2}{2}+z_{i,1}\bar{\alpha}_{i,1}+\frac{5\theta_i\varepsilon_{i,1}}{6}\\&+A_ig_{i,1}z_{i,1}\alpha_{i,1}^{p_{i,1}}+\tilde{\theta}_i\varphi_{i,1}z_{i,1}^2+A_ig_{i,1}z_{i,1}z_{i,2}-\tilde{\theta}_i\dot{\hat{\theta}}_i\Bigg],\end{aligned} \tag{18}$$

where $\bar{\alpha}_{i,1}(x_{i,1},\hat{\theta}_i,y_r)=\frac{c_{i,1}z_{i,1}}{2}+\hat{\theta}_i\varphi_{i,1}z_{i,1}$.

Now, the first virtual controller $\alpha_{i,1}^{p_{i,1}}$ can be chosen as

$$\alpha_{i,1}^{p_{i,1}}(x_{i,1},\hat{\theta}_i,y_r,\rho(t),\dot{\rho}(t))=-Ke-\frac{6\bar{\alpha}_{i,1}^2z_{i,1}}{\bar{g}_{i,1}\sqrt{36z_{i,1}^2\bar{\alpha}_{i,1}^2+\varepsilon_{i,1}^2}}, \tag{19}$$

where K is a positive design parameter, and it leads to

$$\begin{aligned}A_ig_{i,1}z_{i,1}\alpha_{i,1}^{p_{i,1}}&=-A_ig_{i,1}Kez_{i,1}-\frac{6\bar{\alpha}_{i,1}^2}{\sqrt{36z_{i,1}^2\bar{\alpha}_{i,1}^2+\varepsilon_{i,1}^2}}z_{i,1}^2\\&\leq\frac{\theta_i\varepsilon_{i,1}}{6}-z_{i,1}\bar{\alpha}_{i,1}-A_ig_{i,1}Kez_{i,1}.\end{aligned} \tag{20}$$

Finally, combining Equations (16) and (17) yields

$$\begin{aligned}\dot{V}_1 \leq&\sum_{i=1}^{N}\Bigg[-\left(\frac{k_{i,1}z_{i,1}^2}{2}\right)^{\frac{1}{2}}-\frac{c_{i,1}z_{i,1}^2}{2}-A_ig_{i,1}Kez_{i,1}\\&+A_ig_{i,1}z_{i,1}z_{i,2}+\tilde{\theta}_i(\beta_{i,1}-\dot{\hat{\theta}}_i)+2\tilde{\theta}_i\hat{\theta}_i+\theta_i\varepsilon_{i,1}\Bigg],\end{aligned} \tag{21}$$

where $\beta_{i,1}=\varphi_{i,1}z_{i,1}^2-2\hat{\theta}_i$.

According to Lemma 2 and Young's Inequality, we can obtain

$$\begin{aligned}\sum_{i=1}^{N} -A_i g_{i,1} K e z_{i,1} &= -A\underline{g}_1 K z_1^T e = -A\underline{g}_1 K z_1^T (L+B) m \\ &\leq \frac{A\underline{g}_1 K}{2} \lambda_{min}(Q)(\frac{1}{2}\|z_1\|^2 + \frac{1}{2}m^2) \\ &\leq \frac{A\underline{g}_1 K \lambda_{min}(Q)(\|z_1\|^2 + m^2)}{4} \\ &\leq \frac{A\underline{g}_1 K \lambda_{min}(Q)\|z_1\|^2}{2},\end{aligned} \tag{22}$$

where $A = [A_1, A_2, \ldots, A_N]^T$, and $\lambda_{min}(\cdot)$ denotes the minimum eigenvalue of a symmetric positive definite matrix Q.

Substituting Equation (20) into Equation (21) leads to

$$\begin{aligned}\dot{V}_1 \leq \sum_{i=1}^{N} \Bigg[&-\left(\frac{k_{i,1} z_{i,1}^2}{2}\right)^{\frac{1}{2}} - \frac{\bar{c}_{i,1} z_{i,1}^2}{2} + A_i g_{i,1} z_{i,1} z_{i,2} \\ &+ \tilde{\theta}_i(\beta_{i,1} - \dot{\hat{\theta}}_i) + \theta_i \varepsilon_{i,1} + 2\tilde{\theta}_i \hat{\theta}_i \Bigg],\end{aligned} \tag{23}$$

where $\bar{c}_{i,1} = A\underline{g}_1 K \lambda_{min}(Q) + c_{i,1}$.

Step 2: In this step, the Lyapunov function V_2 is chosen as follows

$$V_2 = V_1 + \sum_{i=1}^{N} W_{i,2}(\bar{x}_{i,2}, x_{j,1}, y_r, \hat{\theta}_i, \rho(t), \dot{\rho}(t)). \tag{24}$$

By differentiating V_2 with respect to time, applying Proposition 1, and substituting Equation (21) into Equation (24), it can be deduced that

$$\begin{aligned}\dot{V}_2 \leq \dot{V}_1 + \sum_{i=1}^{N} \Bigg[& g_{i,2} z_{i,2}^{2-\frac{1}{p_{i,1}}} \left(x_{i,3}^{p_{i,2}} - \alpha_{i,2}^{p_{i,2}}\right) + g_{i,2} z_{i,2}^{2-\frac{1}{p_{i,1}}} \alpha_{i,2}^{p_{i,2}} \\ &+ z_{i,2}^{2-\frac{1}{p_{i,1}}} f_{i,2} + z_{i,2}^{2-\frac{1}{p_{i,1}}} d_{i,2} + \left(\frac{k_{i,2} z_{i,2}^2}{2}\right)^{\frac{1}{2}} + \frac{c_{i,2} z_{i,2}^2}{2} \\ &+ \varpi_{i,2} \left(\frac{\partial \alpha_{i,1}^{p_{i,1}}}{\partial x_{i,1}} \dot{x}_{i,1} + \sum_{j=1}^{N} a_{i,j} \frac{\partial \alpha_{i,1}^{p_{i,1}}}{\partial x_{j,1}} \dot{x}_{j,1} + \frac{\partial \alpha_{i,1}^{p_{i,1}}}{\partial y_r} \dot{y}_r \right. \\ &\left. + \frac{\partial \alpha_{i,1}^{p_{i,1}}}{\partial \hat{\theta}_i} \dot{\hat{\theta}}_i + \frac{\partial \alpha_{i,1}^{p_{i,1}}}{\partial \rho} \dot{\rho} + \frac{\partial \alpha_{i,1}^{p_{i,1}}}{\partial \dot{\rho}} \ddot{\rho} \right) \Bigg],\end{aligned} \tag{25}$$

where $\varpi_{i,2} = -\left(2 - \frac{1}{p_{i,1}}\right) \int_{\alpha_{i,1}}^{x_{i,2}} \left(s^{p_{i,1}} - \alpha_{i,1}^{p_{i,1}}\right)^{1-\frac{1}{p_{i,1}}} ds$.

According to Equation (12) and Lemma 5, we can obtain

$$\begin{aligned}& z_{i,2}^{2-\frac{1}{p_{i,1}}} f_{i,2} + z_{i,2}^{2-\frac{1}{p_{i,1}}} d_{i,2} \\ &\leq \frac{2\theta_i \varepsilon_{i,2}}{7} + \theta_i \left(\frac{2p_{i,1}-1}{2p_{i,1}}\right) \left(\gamma_{i,2} \left(\frac{\varepsilon_{i,2}}{7}\right)^{-\frac{1}{2p_{i,1}}}\right)^{\frac{2p_{i,1}}{2p_{i,1}-1}} \\ &\quad + \frac{2p_{i,1}-1}{2p_{i,1}} \left(\gamma_{i,2} \left(\frac{\varepsilon_{i,2}}{7}\right)^{-\frac{1}{2p_{i,1}}}\right)^{\frac{2p_{i,1}}{2p_{i,1}-1}} z_{i,2}^2 \\ &\triangleq \frac{2\theta_i \varepsilon_{i,2}}{7} + \theta_i \varphi_{i,21} z_{i,2}^2,\end{aligned} \tag{26}$$

where $\varphi_{i,21}$ is a smooth positive function.

Furthermore, we have

$$\begin{aligned} & g_{i,1}z_{i,1}z_{i,2}+\left(\frac{k_{i,2}z_{i,2}}{2}\right)^{\frac{1}{2}} \\ & \leq \frac{7\theta_i(1+(1+\bar{g}_{i,1}z_{i,1}^2)^{1/2})^2 z_{i,2}^2}{\sqrt{49(1+(1+\bar{g}_{i,1}z_{i,1}^2)^{1/2})^2)^2+\varepsilon_{i,2}^2}}+\frac{\theta_i\varepsilon_{i,2}}{7} \\ & \triangleq \theta_i\varphi_{i,22}(\bar{x}_{i,2},x_{j,1},y_r,\hat{\theta}_i)z_{i,2}^2+\frac{\theta_i\varepsilon_{i,2}}{7}, \end{aligned} \tag{27}$$

where $\varphi_{i,22}$ is a smooth positive function.

From Lemma 4, it ensures that

$$|x_{i,2}-\alpha_{i,1}| \leq 2^{1-\frac{1}{p_{i,1}}}\left|x_{i,2}^{p_{i,1}}-\alpha_{i,1}^{p_{i,1}}\right|^{\frac{1}{p_{i,1}}}.$$

Thus, we can obtain

$$\begin{aligned} |\varpi_{i,2}| & \leq (2-\frac{1}{p_{i,1}})\,|x_{i,2}-\alpha_{i,1}|\left|x_{i,2}^{p_{i,1}}-\alpha_{i,1}^{p_{i,1}}\right|^{1-\frac{1}{p_{i,1}}} \\ & \leq h_{i,2}\,|z_{i,2}|, \end{aligned} \tag{28}$$

where $h_{i,2}=(2-\frac{1}{p_{i,1}})2^{1-\frac{1}{p_{i,1}}}$.

By using Lemma 3, there exists a smooth positive function $\tilde{\alpha}_{i,2}(x_{i,2},x_{j,1},y_r,\hat{\theta}_i,\rho(t),\dot{\rho}(t))$ such that

$$\begin{aligned} & \left|\frac{\partial\alpha_{i,1}^{p_{i,1}}}{\partial x_{i,1}}\right|+\left|\frac{\partial\alpha_{i,1}^{p_{i,1}}}{\partial x_{j,1}}\right|+\left|\frac{\partial\alpha_{i,1}^{p_{i,1}}}{\partial y_r}\right|+\left|\frac{\partial\alpha_{i,1}^{p_{i,1}}}{\partial\hat{\theta}_i}\right|+\left|\frac{\partial\alpha_{i,1}^{p_{i,1}}}{\partial\rho}\right| \\ & +\left|\frac{\partial\alpha_{i,1}^{p_{i,1}}}{\partial\dot{\rho}}\right| \leq \tilde{\alpha}_{i,2}. \end{aligned} \tag{29}$$

From Assumption 1, Assumption 3, Equations (28) and (29), it can be deduced that

$$\begin{aligned} & \varpi_{i,2}\left(\frac{\partial\alpha_{i,1}^{p_{i,1}}}{\partial y_r}\dot{y}_r+\frac{\partial\alpha_{i,1}^{p_{i,1}}}{\partial x_{j,1}}\dot{x}_{j,1}+\frac{\partial\alpha_{i,1}^{p_{i,1}}}{\partial\rho}\dot{\rho}+\frac{\partial\alpha_{i,1}^{p_{i,1}}}{\partial\dot{\rho}}\ddot{\rho}\right) \\ & \leq \frac{\theta_i 7h_{i,2}^2\tilde{\alpha}_{i,2}^2(H_{i,1}+\gamma_{j,2}+1+(1+\dot{\rho}^2))^2 z_{i,2}^2}{\sqrt{49h_{i,2}^2 z_{i,2}^2\tilde{\alpha}_{i,2}^2(H_{i,1}+\gamma_{j,2}+1+(1+\dot{\rho}^2))^2+\varepsilon_{i,2}^2}} \\ & \quad +\frac{\theta_i\varepsilon_{i,2}}{7} \\ & \triangleq \theta_i\varphi_{i,23}z_{i,2}^2+\frac{\theta_i\varepsilon_{i,2}}{7}, \end{aligned} \tag{30}$$

where $H_{i,1}=(1+\sum_{j=1}^{N}a_{i,j}x_{j,2}^2)^{p_{i,1}/2}$ and $\varphi_{i,23}$ is a smooth positive function.

It can be obtained from Assumption 3, Equations (8) and (27) that

$$\begin{aligned} \varpi_{i,2}\frac{\partial\alpha_{i,1}^{p_{i,1}}}{\partial x_{i,1}}\dot{x}_{i,1} & \leq \frac{7\theta_i h_{i,2}^2\tilde{\alpha}_{i,2}^2(H_{i,2}+\gamma_{i,2})^2 z_{i,2}^2}{\sqrt{49h_{i,2}^2 z_{i,2}^2\tilde{\alpha}_{i,2}^2(H_{i,2}+\gamma_{i,2})^2+\varepsilon_{i,2}^2}} \\ & \quad +\frac{\theta_i\varepsilon_{i,2}}{7} \\ & \triangleq \theta_i\varphi_{i,24}z_{i,2}^2+\frac{\theta_i\varepsilon_{i,2}}{7}, \end{aligned} \tag{31}$$

where $H_{i,2}=(1+x_{i,2}^2)^{p_{i,1}/2}$ and $\varphi_{i,24}$ is a smooth positive function.

Then, it is easy to obtain

$$\begin{aligned}\varpi_{i,2}\frac{\partial\alpha_{i,1}^{p_{i,1}}}{\partial\hat{\theta}_i}\dot{\hat{\theta}}_i &= -\varpi_{i,2}\frac{\partial\alpha_{i,1}^{p_{i,1}}}{\partial\hat{\theta}_i}(\beta_{i,1}-\dot{\hat{\theta}}_i)+\varpi_{i,2}\frac{\partial\alpha_{i,1}^{p_{i,1}}}{\partial\hat{\theta}_i}\beta_{i,1}\\ &\triangleq -\varpi_{i,2}\frac{\partial\alpha_{i,1}^{p_{i,1}}}{\partial\hat{\theta}_i}(\beta_{i,1}-\dot{\hat{\theta}}_i)+\theta_i\tilde{\varphi}_{i,2}z_{i,2}^2\\ &\quad+\frac{\theta_i\varepsilon_{i,2}}{7},\end{aligned}\tag{32}$$

where

$$\tilde{\varphi}_{i,2}(\bar{x}_{i,2},x_{j,1},y_r,\hat{\theta}_i)=\frac{7h_{i,2}^2\tilde{\alpha}_{i,2}^2\beta_{i,1}^2}{\sqrt{49h_{i,2}^2z_{i,2}^2\tilde{\alpha}_{i,2}^2\beta_{i,1}^2+\varepsilon_{i,2}^2}},$$

is a smooth positive function.

The definitions of smooth positive functions are provided below:

$$\begin{aligned}\bar{\varphi}_{i,2}(\bar{x}_{i,2},x_{j,1},y_r,\hat{\theta}_i)&=\sum_{j=1}^{4}\varphi_{i,2j},\\ \varphi_{i,2}(\bar{x}_{i,2},x_{j,1},y_r,\hat{\theta}_i)&=\bar{\varphi}_{i,2}+\tilde{\varphi}_{i,2}.\end{aligned}$$

By substituting Equations (23), (25)–(27) and (30)–(32) into Equation (25), we can obtain

$$\begin{aligned}\dot{V}_2\le&\sum_{i=1}^{N}\sum_{j=1}^{2}\Bigg[-\left(\frac{k_{i,j}z_{i,j}^2}{2}\right)^{\frac{1}{2}}-\frac{\bar{c}_{i,j}z_{i,j}^2}{2}+g_{i,2}z_{i,2}^{2-\frac{1}{p_{i,1}}}\alpha_{i,2}^{p_{i,2}}\\ &+\tilde{\theta}_i(\beta_{i,2}-\dot{\hat{\theta}}_i)+g_{i,2}z_{i,2}^{2-\frac{1}{p_{i,1}}}(x_{i,3}^{p_{i,2}}-\alpha_{i,2}^{p_{i,2}})+\tilde{\theta}_i\varphi_{i,2}z_{i,2}^2\\ &-\varpi_{i,2}\frac{\partial\alpha_{i,1}^{p_{i,1}}}{\partial\hat{\theta}_i}(\beta_{i,2}-\dot{\hat{\theta}}_i)+z_{i,2}\bar{\alpha}_{i,2}+\frac{6\theta_i\varepsilon_{i,2}}{7}+2\tilde{\theta}_i\hat{\theta}_i\\ &+\theta_i\varepsilon_{i,1}\Bigg],\end{aligned}\tag{33}$$

where

$$\bar{\alpha}_{i,2}=h_{i,2}z_{i,2}\tilde{\alpha}_{i,2}\varphi_{i,2}(1+z_{i,2}^2)^{1/2}+\hat{\theta}_i\varphi_{i,2}z_{i,2}+\sum_{i=1}^{N}\frac{c_{i,2}z_{i,2}}{2},$$

and $\beta_{i,2}=\beta_{i,1}+\varphi_{i,2}z_{i,2}^2$.

Design the second virtual controller $\alpha_{i,2}$ as

$$\alpha_{i,2}^{p_{i,2}}(\bar{x}_{i,2},x_{j,1},y_r,\hat{\theta}_i)=-\frac{7\bar{\alpha}_{i,2}^2}{\bar{g}_{i,2}\sqrt{49z_{i,2}^2\bar{\alpha}_{i,2}^2+\varepsilon_{i,2}^2}}z_{i,2}^{1/p_{i,1}},\tag{34}$$

and note that

$$\begin{aligned}g_{i,2}z_{i,2}^{2-\frac{1}{p_{i,1}}}\alpha_{i,2}^{p_{i,2}}&=-\frac{7z_{i,2}^2\bar{\alpha}_{i,2}^2}{\sqrt{49z_{i,2}^2\bar{\alpha}_{i,2}^2+\varepsilon_{i,2}^2}}\\ &\le\frac{\theta_i\varepsilon_{i,2}}{7}-z_{i,2}\bar{\alpha}_{i,2}.\end{aligned}\tag{35}$$

Finally, a direct calculation indicates that

$$\begin{aligned}\dot{V}_2 \leq & \sum_{i=1}^{N}\sum_{j=1}^{2}\Big[-\left(\frac{k_{i,j}z_{i,j}^2}{2}\right)^{\frac{1}{2}} - \left(\frac{\bar{c}_{i,j}z_{i,j}^2}{2}\right) + \tilde{\theta}_i(\beta_{i,2} - \dot{\hat{\theta}}_i) \\ & + 2\tilde{\theta}_i\hat{\theta}_i + 2\theta_i\varepsilon_{i,j} + g_{i,2}z_{i,2}^{2-\frac{1}{p_{i,1}}}(x_{i,3}^{p_{i,2}} - \alpha_{i,2}^{p_{i,2}}) \\ & - \varpi_{i,2}\frac{\partial\alpha_{i,1}^{p_{i,1}}}{\partial\hat{\theta}_i}(\beta_{i,2} - \dot{\hat{\theta}}_i)\Big].\end{aligned} \tag{36}$$

Step k (k = 3,4,...,n): Assume that at step $k-1$, there exists a virtual controller $\alpha_{i,k-1}$ such that the time derivative of a continuously differentiable function V_{k-1} satisfies

$$\begin{aligned}\dot{V}_{k-1} \leq & \sum_{i=1}^{N}\sum_{j=1}^{k-1}\Bigg[-\left(\frac{k_{i,j}z_{i,j}^2}{2}\right)^{\frac{1}{2}} - \frac{\bar{c}_{i,j}z_{i,j}^2}{2} + \tilde{\theta}_i(\beta_{i,k-1} - \dot{\hat{\theta}}_i) \\ & + 2\tilde{\theta}_i\hat{\theta}_i - \sum_{j=1}^{k-2}\varpi_{i,j+1}\frac{\partial\alpha_{i,j}^{p_{i,1}\cdots\cdots p_{i,j}}}{\partial\hat{\theta}_i}(\beta_{i,k-1} - \dot{\hat{\theta}}_i) \\ & + g_{i,k}z_{i,k-1}^{2-\frac{1}{p_{i,1}\cdots p_{i,k-2}}}(x_{i,k}^{p_{i,k-1}} - \alpha_{i,k-1}^{p_{i,k-1}}) \\ & + (k-1)\theta_i\varepsilon_{i,j}\Bigg],\end{aligned} \tag{37}$$

where $\beta_{i,k-1} = \sum_{i=1}^{N}\sum_{j=1}^{k-1}(\varphi_{i,j}z_{i,j}^2 - 2\hat{\theta}_i)$, $\varphi_{i,j}(j = 1,2,\ldots,k-1)$ are smooth positive functions with specified definitions, and $\varpi_{i,j+1}(j = 1,2,\ldots,k-1)$ represent continuous functions.

In this step, the aim is to appropriately select the virtual controller $\alpha_{i,k}$.

We define

$$V_k = V_{k-1} + W_{i,k}(\bar{x}_{i,k-1}, \bar{x}_{j,k-1}, y_r, \hat{\theta}_i). \tag{38}$$

Then, by using Equation (38) in the time derivative of V_k, and based on Proposition 1, we have

$$\begin{aligned}\dot{V}_k \leq & \sum_{i=1}^{N}\sum_{j=1}^{k-1}\Bigg[-\left(\frac{k_{i,j}z_{i,j}^2}{2}\right)^{\frac{1}{2}} - \frac{\bar{c}_{i,j}z_{i,j}^2}{2} + \frac{c_{i,k}z_{i,k}^2}{2} + 2\tilde{\theta}_i\hat{\theta}_i \\ & +\tilde{\theta}_i(\beta_{i,k-1} - \dot{\hat{\theta}}_i)\Bigg] + (k-1)\theta_i\varepsilon_{i,j} + \left(\frac{k_{i,k}z_{i,k}^2}{2}\right)^{\frac{1}{2}} \\ & + g_{i,k-1}z_{i,k-1}^{2-\frac{1}{p_{i,1}\cdots p_{i,k-2}}}(x_{i,k}^{p_{i,k-1}} - \alpha_{i,k-1}^{p_{i,k-1}}) \\ & + g_{i,k}z_{i,k}^{2-\frac{1}{p_{i,1}\cdots p_{i,k-1}}}\alpha_{i,k}^{p_{i,k}} + \tilde{\theta}_i(\beta_{i,k-1} - \dot{\hat{\theta}}_i) \\ & + g_{i,k}z_{i,k}^{2-\frac{1}{p_{i,1}\cdots p_{i,k-1}}}(x_{i,k+1}^{p_{i,k}} - \alpha_{i,k}^{p_{i,k}}) \\ & + \varpi_{i,k}\Bigg(\frac{\partial\alpha_{i,k-1}^{p_{i,1}\cdots p_{i,k-1}}}{\partial x_{i,j}}\dot{x}_{i,j} + \frac{\partial\alpha_{i,k-1}^{p_{i,1}\cdots p_{i,k-1}}}{\partial y_r}\dot{y}_r \\ & + \frac{\partial\alpha_{i,k-1}^{p_{i,1}\cdots p_{i,k-1}}}{\partial\hat{\theta}_i}\dot{\hat{\theta}}_i + \sum_{j=1}^{N}a_{i,j}\sum_{l=1}^{k-1}\frac{\partial\alpha_{i,k-1}^{p_{i,1}\cdots p_{i,k-1}}}{\partial x_{j,l}}\dot{x}_{j,l}\Bigg) \\ & + z_{i,k}^{2-\frac{1}{p_{i,1}\cdots p_{i,k-1}}}f_{i,k} + z_{i,k}^{2-\frac{1}{p_{i,1}\cdots p_{i,k-1}}}d_{i,k},\end{aligned} \tag{39}$$

where

$$\begin{aligned}\varpi_{i,k} = & -\int_{\alpha_{i,k-1}}^{x_{i,k}}(s^{p_{i,1}\cdots p_{i,k-1}} - \alpha_{i,k-1}^{p_{i,1}\cdots p_{i,k-1}})^{1-\frac{1}{p_{i,1}\cdots p_{i,k-1}}}ds \\ & \cdot(2 - \frac{1}{p_{i,1}\cdots p_{i,k-1}}).\end{aligned}$$

In the following, one needs to properly estimate the destabilizing terms on the right-hand side of Equation (39). Using Lemma 5, it can be deduced that

$$\begin{aligned} & z_{i,k}^{2-\frac{1}{p_{i,1}\cdots p_{i,k-1}}} f_{i,k} + z_{i,k}^{2-\frac{1}{p_{i,1}\cdots p_{i,k-1}}} d_{i,k} \\ & \leq \frac{\theta_i \varepsilon_{i,k}}{9} + \frac{H_{i,3}\theta_i z_{i,k}^2}{H_{i,3}+1} (\gamma_{i,k} (\frac{\varepsilon_{i,k}}{9})^{-\frac{1}{H_{i,3}}})^{\frac{H_{i,3}+1}{H_{i,3}}} \\ & \triangleq \frac{2\theta_i \varepsilon_{i,k}}{9} + \theta_i \varphi_{i,k1} z_{i,k}^2, \end{aligned} \tag{40}$$

where $H_{i,3} = 2p_{i,1} \dots p_{i,k-1} - 1$ and $\varphi_{i,k1}$ is a smooth positive function.

From Assumption 2 and Lemmas 1 and 4, we have:

$$\begin{aligned} & g_{i,k-1} z_{i,k-1}^{2-\frac{1}{p_{i,1}\cdots p_{i,k-1}}} (x_{i,k}^{p_{i,k-1}} - \alpha_{i,k-1}^{p_{i,k-1}}) + \sum_{i=1}^{N} \left(\frac{k_{i,k} z_{i,k}^2}{2} \right)^{\frac{1}{2}} \\ & \leq \frac{2^{1-\frac{1}{p_{i,1}\cdots p_{i,k-2}}} \theta_i z_{i,k}^2}{2p_{i,1}\dots p_{i,k-2}} \left(\frac{9 z_{i,k-1}^2}{\varepsilon_{i,k}} \right)^{2p_{i,1}\dots p_{i,k-2}-1} + \frac{\theta_i \varepsilon_{i,k}}{3} \\ & \triangleq \theta_i \varphi_{i,k2} z_{i,k}^2 + \frac{\theta_i \varepsilon_{i,k}}{3}, \end{aligned} \tag{41}$$

where $\varphi_{i,k2}$ is a smooth positive function.

From Lemma 4, it ensures that

$$|x_{i,k} - \alpha_{i,k-1}| \leq 2^{1-\frac{1}{p_{i,1}\cdots p_{i,k-1}}} |z_{i,k}|^{\frac{1}{p_{i,1}\cdots p_{i,k-1}}},$$

which further implies

$$\begin{aligned} |\varpi_{i,k}| & \leq (2 - \frac{1}{p_{i,1}\cdots p_{i,k-1}}) |x_{i,k} - \alpha_{i,k-1}| |z_{i,k}|^{1-\frac{1}{p_{i,1}\cdots p_{i,k-1}}} \\ & \leq h_{i,k} |z_{i,k}|, \end{aligned} \tag{42}$$

where $h_{i,k} = (2 - \frac{1}{p_{i,1}\cdots p_{i,k-1}}) 2^{1-\frac{1}{p_{i,1}\cdots p_{i,k-1}}}$ is a positive constant.

By using Lemma 3, there exists a smooth positive function $\tilde{\alpha}_{i,k}(\bar{x}_{i,k-1}, rx_{j,k-1}, y_r, \hat{\theta}_i)$ such that

$$\begin{aligned} & \sum_{i=1}^{N} \left| \frac{\partial \alpha_{i,k-1}^{p_{i,1}\cdots p_{i,k-1}}}{\partial x_{i,j}} \right| + \sum_{j=1}^{N} a_{i,j} \sum_{l=1}^{k-1} \left| \frac{\partial \alpha_{i,k-1}^{p_{i,1}\cdots p_{i,k-1}}}{\partial x_{j,l}} \right| \\ & + \left| \frac{\partial \alpha_{i,k-1}^{p_{i,1}\cdots p_{i,k-1}}}{\partial y_r} \right| + \left| \frac{\partial \alpha_{i,k-1}^{p_{i,1}\cdots p_{i,k-1}}}{\partial \hat{\theta}_j} \right| \leq \tilde{\alpha}_{i,k}. \end{aligned} \tag{43}$$

From Assumption 1, Assumption 3, Equations (42) and (43), it can be deduced that

$$\begin{aligned} & \varpi_{i,k} \left(\frac{\partial \alpha_{i,k-1}^{p_{i,1}\cdots p_{i,k-1}}}{\partial y_r} \dot{y}_r + \sum_{j=1}^{N} a_{i,j} \sum_{l=1}^{k-1} \frac{\partial \alpha_{i,k-1}^{p_{i,1}\cdots p_{i,k-1}}}{\partial x_{j,l}} \dot{x}_{j,l} \right) \\ & \leq \frac{9 h_{i,k}^2 \tilde{\alpha}_{i,k}^2 \theta_i \left((H_{i,4})^{p_{i,k-1}/2} + \gamma_{j,k} + 1 \right)^2 z_{i,k}^2}{\sqrt{64 h_{i,k}^2 z_{i,k}^2 \tilde{\alpha}_{i,k}^2 \left((H_{i,4})^{p_{i,k-1}/2} + \gamma_{j,k} + 1 \right)^2 + \varepsilon_{i,k}^2}} \\ & + \frac{\theta_i \varepsilon_{i,k}}{9} \\ & \triangleq \theta_i \varphi_{i,k3} (\bar{x}_{i,k-1}, \bar{x}_{j,k-1}, y_r, \hat{\theta}_i) z_{i,k}^2 + \frac{\theta_i \varepsilon_{i,k}}{9}, \end{aligned} \tag{44}$$

where $\varphi_{i,k3}$ is a smooth positive function, and $H_{i,4} = 1 + \sum_{j=1}^{N} a_{ij} \sum_{l=1}^{k-1} x_{j,l}^2$.

It can be evaluated from Assumption 3, Equations (11) and (45) that

$$
\begin{aligned}
&\varpi_{i,k}\sum_{j=1}^{k-1}\frac{\partial\alpha_{i,k-1}^{p_{i,1}\cdots p_{i,k-1}}}{\partial x_{i,j}}\dot{x}_{i,j}\\
&\leq\frac{9h_{i,k}^2\tilde{\alpha}_{i,k}^2\theta_i\left((1+\sum\limits_{j=1}^{k-1}x_{i,j}^2)^{p_{i,k-1}/2}+\gamma_{i,k}\right)^2 z_{i,k}^2}{\sqrt{81h_{i,k}^2z_{i,k}^2\tilde{\alpha}_{i,k}^2\left((1+\sum\limits_{j=1}^{k-1}x_{i,j}^2)^{p_{i,k-1}/2}+\gamma_{i,k}\right)^2+\varepsilon_{i,k}^2}}\\
&\quad+\frac{\theta_i\varepsilon_{i,k}}{9}\\
&\triangleq\theta_i\varphi_{k,k2}(\bar{x}_{i,k-1},\bar{x}_{j,k-1},y_r,\hat{\theta}_i)z_{i,k}^2+\frac{\theta_i\varepsilon_{i,k}}{9},
\end{aligned}
\tag{45}
$$

where $\varphi_{i,k4}$ is a smooth positive function.

Similar to step 2, it is easy to obtain

$$
\begin{aligned}
\varpi_{i,k}\frac{\partial\alpha_{i,k-1}^{p_{i,1}\cdots p_{i,k-1}}}{\partial\hat{\theta}_i}\dot{\hat{\theta}}_i&=-\varpi_{i,k}\frac{\partial\alpha_{i,k-1}^{p_{i,1}\cdots p_{i,k-1}}}{\partial\hat{\theta}_i}(\beta_{i,k-1}-\dot{\hat{\theta}}_i)\\
&\quad+\varpi_{i,k}\frac{\partial\alpha_{i,k-1}^{p_{i,1}\cdots p_{i,k-1}}}{\partial\hat{\theta}_i}\beta_{i,k-1}\\
&\triangleq-\varpi_{i,k}\frac{\partial\alpha_{i,k-1}^{p_{i,1}\cdots p_{i,k-1}}}{\partial\hat{\theta}_i}(\beta_{i,k-1}-\dot{\hat{\theta}}_i)\\
&\quad+\theta_i\tilde{\varphi}_{i,k}z_{i,k}^2+\frac{\theta_i\varepsilon_{i,k}}{9},
\end{aligned}
\tag{46}
$$

where

$$
\tilde{\varphi}_{i,k}(\bar{x}_{i,k-1},\bar{x}_{j,k-1},y_r,\hat{\theta}_i)=\frac{9h_{i,k}^2\tilde{\alpha}_{i,k}^2\beta_{i,k-1}^2}{\sqrt{81h_{i,k}^2z_{i,k}^2\tilde{\alpha}_{i,k}^2\beta_{i,k-1}^2+\varepsilon_{i,k}^2}},
$$

is a smooth positive function.

Among these, the following definitions of smooth positive functions are presented:

$$
\begin{aligned}
\bar{\varphi}_{i,k}(\bar{x}_{i,k-1},\bar{x}_{j,k-1},y_r,\hat{\theta}_i)&=\sum_{j=1}^{4}\varphi_{i,kj},\\
\varphi_{i,j}(\bar{x}_{i,k-1},\bar{x}_{j,k-1},y_r,\hat{\theta}_i)&=\bar{\varphi}_{i,k}+\tilde{\varphi}_{i,k}.
\end{aligned}
$$

Substituting Equations (34), (35), and (43)–(45) into Equation (37), we have

$$
\begin{aligned}
\dot{V}_k\leq&\sum_{i=1}^{k-1}\sum_{j=1}^{k-1}\Bigg[-\left(\frac{k_{i,j}z_{i,j}^2}{2}\right)^{\frac{1}{2}}-\frac{\bar{c}_{i,j}z_{i,j}^2}{2}+(k-1)\theta_i\varepsilon_{i,j}\\
&+2\tilde{\theta}_i\hat{\theta}_i+\frac{8\theta_i\varepsilon_{i,k}}{9}+\tilde{\theta}_i(\beta_{i,k}-\dot{\hat{\theta}}_i)+z_{i,k}\bar{\alpha}_{i,k}\\
&+g_{i,k}z_{i,k}^{2-\frac{1}{p_{i,1}\cdots p_{i,k-1}}}\alpha_{i,k}^{p_{i,k}}+\tilde{\theta}_i\varphi_{i,k}z_{i,k}^2\\
&+g_{i,k}z_{i,k}^{2-\frac{1}{p_{i,1}\cdots p_{i,k-1}}}(x_{i,k+1}^{p_{i,k}}-\alpha_{i,k}^{p_{i,k}})\\
&-\varpi_{i,j}\frac{\partial\alpha_{i,k-1}^{p_{i,1}\cdots p_{i,k-1}}}{\partial\hat{\theta}_i}(\beta_{i,k}-\dot{\hat{\theta}}_i)\Bigg],
\end{aligned}
\tag{47}
$$

where $\beta_{i,k}=\beta_{i,k-1}+\varphi_{i,k}z_{i,k}^2$, and

$$
\begin{aligned}
\bar{\alpha}_{i,k}(\bar{x}_{i,k},\bar{x}_{j,k-1},y_r,\hat{\theta}_i)=&h_{i,k}z_{i,k}\tilde{\alpha}_{i,k}(1+z_{i,k}^2)^{1/2}h_{i,k}\\
&+\hat{\theta}_ih_{i,k}z_{i,k}+\sum_{i=1}^{N}\frac{c_{i,k}z_{i,k}}{2}.
\end{aligned}
$$

Now, the k-th virtual controller $\alpha_{i,k}$ can be constructed to satisfy

$$\alpha_{i,k}^{p_{i,k}}(\bar{x}_{i,k},\bar{x}_{j,k-1},y_r,\hat{\theta}_i)=-\frac{9\bar{\alpha}_{i,k}^2 z_{i,k}^{1/p_{i,1}\cdots p_{i,k-1}}}{\bar{g}_{i,k}\sqrt{81z_{i,k}^2\bar{\alpha}_{i,k}^2+\varepsilon_{i,k}^2}}, \tag{48}$$

which demonstrates that

$$\begin{aligned} g_{i,k}z_{i,k}^{2-\frac{1}{p_{i,1}\cdots p_{i,k-1}}}\alpha_{i,k}^{p_{i,k}} &= -\frac{9z_{i,k}^2\bar{\alpha}_{i,k}^2}{\sqrt{81z_{i,k}^2\bar{\alpha}_{i,k}^2+\varepsilon_{i,k}^2}} \\ &\le \frac{\theta_i\varepsilon_{i,k}}{9}-z_{i,k}\bar{\alpha}_{i,k}. \end{aligned} \tag{49}$$

Finally, we have

$$\begin{aligned} \dot{V}_k \le & \sum_{i=1}^{N}\sum_{j=1}^{k}\Bigg[-\left(\frac{k_{i,j}z_{i,j}^2}{2}\right)^{\frac{1}{2}}-\frac{\bar{c}_{i,j}z_{i,j}^2}{2}+2\tilde{\theta}_i\hat{\theta}_i+k\theta_i\varepsilon_{i,j} \\ & +\tilde{\theta}_i(\beta_{i,k}-\dot{\hat{\theta}}_i)+g_{i,k}z_{i,k}^{2-\frac{1}{p_{i,1}\cdots p_{i,k-1}}}(x_{i,k+1}^{p_{i,k}}-\alpha_{i,k}^{p_{i,k}}) \\ & -\varpi_{i,j}\frac{\partial\alpha_{i,k-1}^{p_{i,1}\cdots p_{i,k-1}}}{\partial\hat{\theta}_i}(\beta_{i,k}-\dot{\hat{\theta}}_i)\Bigg]. \end{aligned} \tag{50}$$

Note that Equation (50) still holds for $k=n$

$$\begin{aligned} \dot{V}_n \le & \sum_{i=1}^{N}\sum_{j=1}^{n}\Bigg[-\left(\frac{k_{i,j}z_{i,j}^2}{2}\right)^{\frac{1}{2}}-\frac{\bar{c}_{i,j}z_{i,j}^2}{2}+2\tilde{\theta}_i\hat{\theta}_i+k\theta_i\varepsilon_{i,j} \\ & +\tilde{\theta}_i(\beta_{i,n}-\dot{\hat{\theta}}_i)+g_{i,n}z_{i,n}^{2-\frac{1}{p_{i,1}\cdots p_{i,n-1}}}(u_i^{p_{i,n}}-\alpha_{i,n}^{p_{i,n}}) \\ & -\varpi_{i,j}\frac{\partial\alpha_{i,n-1}^{p_{i,1}\cdots p_{i,n-1}}}{\partial\hat{\theta}_i}(\beta_{i,n}-\dot{\hat{\theta}}_i)\Bigg], \end{aligned} \tag{51}$$

where $\beta_{i,\mathrm{n}}=\beta_{i,n-1}+\varphi_{i,n}z_{i,n}^2$.

Now, the adaptive law can be designed as follows:

$$\dot{\hat{\theta}}_i=\beta_{i,\mathrm{n}}. \tag{52}$$

The controller is designed as

$$u_i^{p_{i,n}}=-\frac{9\bar{\alpha}_{i,n}^2}{\bar{g}_{i,n}\sqrt{81z_{i,n}^2\bar{\alpha}_{i,n}^2+\varepsilon_{i,n}^2}}z_{i,n}^{1/p_{i,1}\cdots p_{i,n-1}}. \tag{53}$$

From Equations (52) and (53), we have

$$\dot{V}_n\le\sum_{i=1}^{N}\sum_{j=1}^{n}\Bigg[-\left(\frac{k_{i,j}z_{i,j}^2}{2}\right)^{\frac{1}{2}}-\frac{\bar{c}_{i,j}z_{i,j}^2}{2}+2\tilde{\theta}_i\hat{\theta}_i+k\theta_i\varepsilon_{i,j}\Bigg]. \tag{54}$$

4. Stability Analysis

Theorem 1. *Consider the high-power nonlinear MASs (1)–(2) under Assumptions 1-4, if the initial tracking error satisfies* $|m_i(0)|<\rho(0)$*, then the proposed control scheme, which integrates virtual controllers (19), (34) and (48), the actual controller (53), as well as the adaptive law (52), possesses the following properties: (i) all signals in the closed-loop system remain bounded; (ii) the tracking error is confined within a predefined bound and converges to a predefined accuracy within a prescribed time.*

Proof. According to Young's inequality, we have

$$2\tilde{\theta}_i\hat{\theta}_i \leq -\frac{\tilde{\theta}_i^2}{2} - [\frac{\left|\tilde{\theta}_i\right|}{2} - \frac{1}{2}]^2 - (\frac{\tilde{\theta}_i^2}{2})^{\frac{1}{2}} + \frac{1}{2} + \theta_i^2 \\ \leq -\frac{\tilde{\theta}_i^2}{2} - (\frac{\tilde{\theta}_i^2}{2})^{\frac{1}{2}} + \frac{1}{2} + \theta_i^2. \tag{55}$$

Combining Equations (54) and (55), there is

$$\dot{V}_n \leq \sum_{i=1}^{N}\sum_{j=1}^{n}[-\left(\frac{k_{i,j}z_{i,j}^2}{2}\right)^{\frac{1}{2}} - \frac{\bar{c}_{i,j}z_{i,j}^2}{2} - \frac{\tilde{\theta}_i^2}{2} - (\frac{\tilde{\theta}_i^2}{2})^{\frac{1}{2}} + \rho_i], \tag{56}$$

where $\rho_i = \frac{1}{2} + \sum\limits_{i=1}^{N}\sum\limits_{j=1}^{n}(\theta_i^2 + k\theta_i\varepsilon_{i,j})$. Similar to the deduction of (42), there is $W_{i,n} \leq 2^{1-\frac{1}{p_{i,1}\cdots p_{i,n-1}}} z_{i,n}^2 \leq 2z_{i,n}^2$, and combined with Equation (56) and Lemma 6, we can obtain

$$\dot{V}_n \leq \sum_{i=1}^{N}\sum_{j=1}^{n}[-\left(\frac{k_{i,j}z_{i,j}^2}{2} + \frac{\tilde{\theta}_i^2}{2}\right)^{\frac{1}{2}} - (\frac{\bar{c}_{i,j}z_{i,j}^2}{2} + \frac{\tilde{\theta}_i^2}{2}) + \rho_i] \\ \leq -aV_n^{\frac{1}{2}} - bV_n + \bar{\rho}, \tag{57}$$

where the constants a and b are related to the positive constants $k_{i,j}$ and $\bar{c}_{i,j}$, and $\bar{\rho} = \sum\limits_{i=1}^{N}\sum\limits_{j=1}^{n}\rho_i$.

From Lemma 7 and Equation (57), we can obtain the boundedness of V_n for $i = 1, 2, \ldots, n$, which suggests that $m_i(t)$, $e_i(t)$, $z_{i,j}(t)$ and $\tilde{\theta}_i(t)$ are all bounded within finite time. In addition, by ensuring the boundedness of $\tilde{\theta}_i(t)$ and $\theta_i(t)$, it is guaranteed that $\hat{\theta}_i(t)$ is bounded. Using the boundedness of $m_{i,1}(t)$, and $m_{i,1}(t) = x_{i,1}(t) - y_r(t)$, it can be concluded that $x_{i,1}(t)$ is also bounded. Through the barrier function (8) and the boundedness of z_1, it is ensured that $|e|$ remains strictly smaller than the performance function (7). Therefore, it has been established that all states of the closed-loop system are bounded. □

5. Simulation Example

In this section, the effectiveness of the theoretical results is illustrated using an example of leader-following MASs composed of three follower agents and one leader agent. The communication network is depicted in Figure 1, which illustrates the communication topology of the nonlinear MASs. In Figure 1, the node labeled as y_r represents the leader, and those nodes numbered 1 to 3 represent the followers. Notably, the leader's signal is exclusively received by follower 1. The corresponding weight matrix between the leader and the followers is $B = \text{diag}(1, 0, 0)$. The adjacency matrix A and the Laplacian matrix L of the following agents are $A = \begin{pmatrix} 0 & 0 & 0 \\ 1 & 0 & 0 \\ 0 & 1 & 0 \end{pmatrix}$ and $L = \begin{pmatrix} 0 & 0 & 0 \\ -1 & 1 & 0 \\ 0 & -1 & 1 \end{pmatrix}$, respectively.

To demonstrate the effectiveness of the proposed control mechanism, the following nonlinear high-power MASs are introduced:

$$\begin{cases} \dot{x}_{i,1} = x_{i,2}^{p_{i,1}} + \sin(0.5x_{i,1}) + 0.05\cos(t), \\ \dot{x}_{i,2} = u_i + \cos(0.5x_{i,1}) - 0.02\sin(0.05x_{i,2}) + 0.05\cos(t), \end{cases} \tag{61}$$

where $i = 1, 2, 3$.

The leader's dynamics is given by

$$\begin{cases} \dot{y}_r = 1.512\cos(0.63 - 1.1) + 0.0005\cos(0.01t + 1.5), \\ x_r = y_r. \end{cases} \tag{62}$$

The control objective is to ensure that the output signal $y_i(t)$ tracks the reference signal $y_r(t)$. In accordance with the control scheme presented in this paper, the parameters are selected as follows: The initial values are selected as $x(0) = [x_1(0), x_2(0), x_3(0)] = [0.8, 0.1, 5]$, $\theta_1(0) = 5$, $\theta_2(0) = 5$ and $\theta_3(0) = 5$. The design parameters are given as $K = 0.01, p_{11} = p_{21} = p_{31} = 1, k_{11} = k_{21} = k_{31} = 2, \varepsilon_{11} = \varepsilon_{21} = \varepsilon_{31} = 50, \varepsilon_{12} =$

$\varepsilon_{22} = \varepsilon_{32} = 1500, c_{11} = c_{21} = c_{31} = 40$ and $c_{12} = c_{22} = c_{32} = 0.01$, $\rho_t r = 0.68, l = 0.001, J = 1.8$, $q_1 = q_2 = q_3 = 0.5, \bar{\sigma}_1 = 0.01, \bar{\sigma}_2 = 0.005, \bar{\sigma}_3 = 0.02$. In addition, the virtual control function $\alpha_{i,1}$, the parameter adaptive law $\hat{\theta}_i$ and the actual control signal u_i are constructed in Equations (19), (52), and (53), respectively. In the simulation, the initial conditions are taken as $x_r(0) = 1.06$, $x_1(0) = [0.8, 0.1]^T$, $x_2(0) = [0.82, 0.1]^T$, $x_3(0) = [0.78, 0.1]^T$, and $\hat{\theta}_i(0) = 5$ for $i = 1, 2, 3$. The simulation is conducted with three sets of different design parameters, all under the same initial conditions.

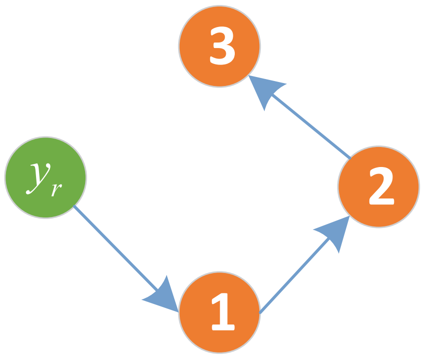

Figure 1. The topology of the communication graph.

The simulation results are presented in Figures 2–5. The output of each subsequent agent successfully follows the desired trajectory of the leader, as illustrated in Figure 2, and Figure 3 depicts the variation of the tracking error trajectory over time. From Figure 3, it can be observed that the tracking error remains within the prescribed bounds and satisfies $-0.705 < e(t) < 0.705$ for $t \geq 2$. Given that the tracking error is strictly confined to the interval $[-\rho, \rho]$, the consensus error is consequently bounded within the same range, which is clearly indicated by the experimental curves in Figure 3. The trajectory of the adaptive parameter $\hat{\theta}_i$ is shown in Figure 4. The actual controller trajectory is illustrated in Figure 5. The simulation results indicate that the proposed tracking control mechanism ensures consensus tracking for the considered MASs.

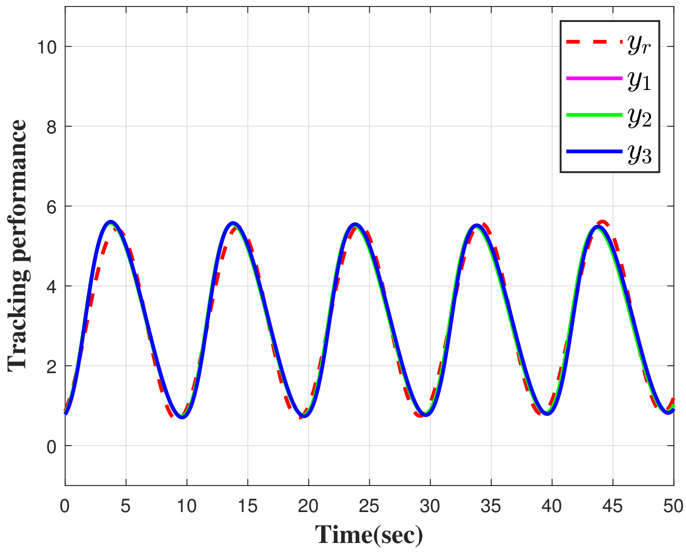

Figure 2. Output trajectories of three followers and one leader.

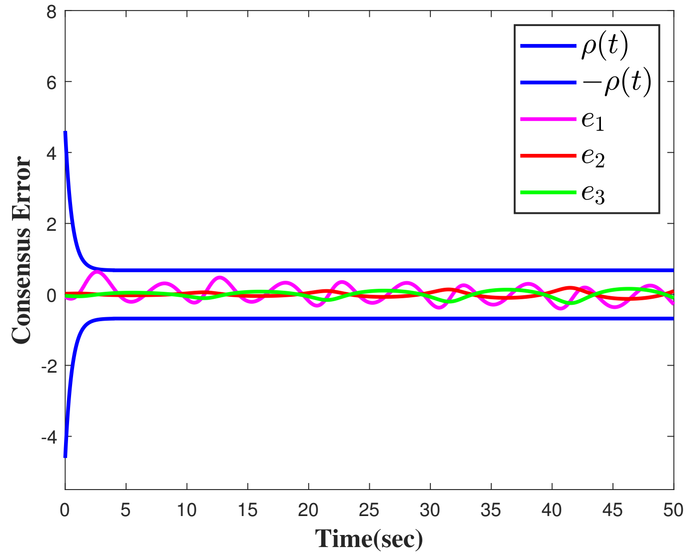

Figure 3. Tracking error and performance envelope.

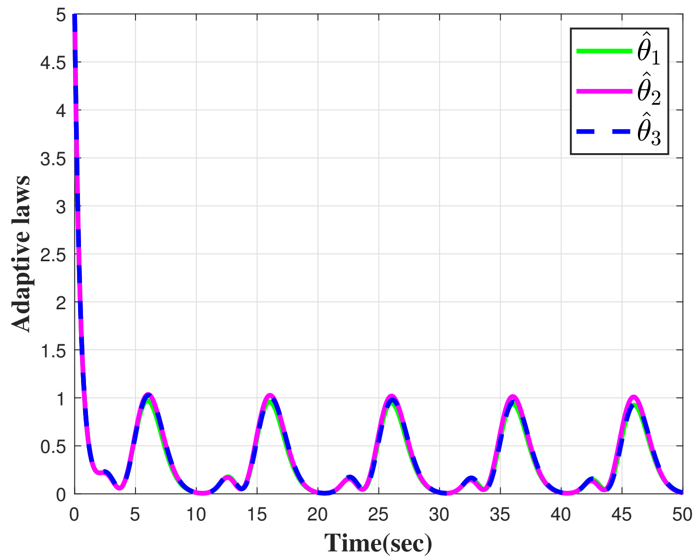

Figure 4. The adaptive laws of parameters $\hat{\theta}_i$.

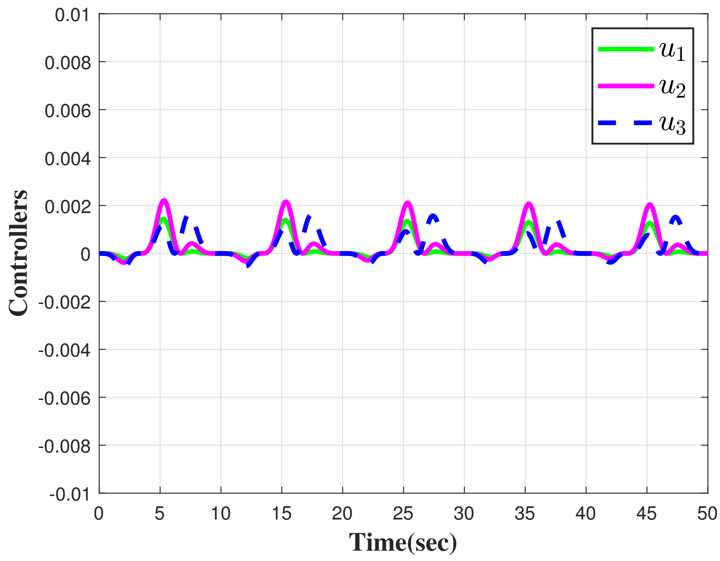

Figure 5. Controller signals u_i.

6. Conclusions

This paper presents the study and design of a novel adaptive consensus tracking control mechanism aimed at addressing the challenges of fast finite-time tracking control and prescribed performance control under external signal disturbances in high-power uncertain nonlinear MASs. Compared to traditional methods, the proposed control mechanism not only guarantees the asymptotic convergence of the output of the MASs but also enhances the system's performance during both transient and steady-state stages by incorporating a prescribed performance function. Moreover, the designed finite-time control framework meets the system's performance requirements within a finite time. Future work may focus on optimizing controller design to improve the system's robustness in more complex environments, investigating adaptive control strategies based on dynamic event-triggered mechanisms, and addressing global coordination and security issues in MASs.

Author Contributions

X.Z.(Xiao Zheng): conceptualization, methodology, writing—original draft preparation; Y.C.: data curation; X.Z.(Xiaoqing Zhang): visualization, investigation; X.W.: supervision; Y.N.: writing—reviewing and editing. All authors have read and agreed to the published version of the manuscript.

Funding

This work was supported by National Natural Science Foundation of China (Grant 62406178), by China Postdoctoral Science Foundation (Grant 2025M771718), by Postdoctoral Fellowship Program of China Postdoctoral Science Foundation (Grant GZC20251189), by Natural Science Foundation of Chongqing (Grant CSTB2025NSCO-GPX0746), and by Natural Science Foundation of Shandong Province (Grant ZR2024MF091).

Conflicts of Interest

The authors declare no conflict of interest.

References

1. Qamar, S.; Khan, S.H.; Arshad, M.A.; et al. Autonomous drone swarm navigation and multitarget tracking with island policy-based optimization framework. *IEEE Access* **2022**, *10*, 91073–91091.
2. Das, S.; Goswami, D.; Chatterjee, S.; et al. Stability and chaos analysis of a novel swarm dynamics with applications to multi-agent systems. *Eng. Appl. Artif. Intell.* **2014**, *30*, 189–198.
3. Han, L.; Wang, Y.; Yan, Z.; et al. Event-triggered formation control with obstacle avoidance for multi-agent systems applied to multi-UAV formation flying. *Control. Eng. Pract.* **2024**, *153*, 106105.
4. Li, Z.; Duan, Z.; Lewis, F.L. Distributed robust consensus control of multi-agent systems with heterogeneous matching uncertainties. *Automatica* **2014**, *50*, 883–889.
5. Wen, G.; Wang, H.; Yu, X.; et al. Bipartite tracking consensus of linear multi-agent systems with a dynamic leader. *IEEE Trans. Circuits Syst. II Express Br.* **2017**, *65*, 1204–1208.
6. Zhang, P.; Xue, H.; Gao, S.; et al. Distributed adaptive consensus tracking control for multi-agent system with communication constraints. *IEEE Trans. Parallel Distrib. Syst.* **2020**, *32*, 1293–1306.
7. Zhang, L.; Che, W.W.; Chen, B.; et al. Adaptive fuzzy output-feedback consensus tracking control of nonlinear multiagent systems in prescribed performance. *IEEE Trans. Cybern.* **2022**, *53*, 1932–1943.
8. Zhao, X.; Shi, P.; Zheng, X.; et al. Intelligent tracking control for a class of uncertain high-order nonlinear systems. *IEEE Trans. Neural Netw. Learn. Syst.* **2015**, *27*, 1976–1982.
9. Zhao, Y.; Zhou, Y.; Zhong, Z.; et al. Distributed optimal cooperation for multiple high-order nonlinear systems with Lipschitz-type gradients: Static and adaptive state-dependent designs. *IEEE Trans. Syst. Man Cybern. Syst.* **2021**, *52*, 5378–5388.
10. Wang, H.; Ma, J.; Zhao, X.; et al. Adaptive fuzzy fixed-time control for high-order nonlinear systems with sensor and actuator faults. *IEEE Trans. Fuzzy Syst.* **2023**, *31*, 2658–2668.
11. Min, H.; Xu, S.; Gu, J.; et al. Further results on adaptive stabilization of high-order stochastic nonlinear systems subject to uncertainties. *IEEE Trans. Neural Netw. Learn. Syst.* **2019**, *31*, 225–234.
12. Yue, D.; Deng, C.; Wen, C.; et al. Finite-time distributed resilient tracking control for nonlinear MASs with application to power systems. *IEEE Trans. Autom. Control.* **2023**, *69*, 3128–3143.
13. Lan, J.; Liu, Y.J.; Xu, T.; et al. Adaptive fuzzy fast finite-time formation control for second-order MASs based on capability boundaries of agents. *IEEE Trans. Fuzzy Syst.* **2021**, *30*, 3905–3917.
14. Shang, Z.; Jiang, Y.; Niu, B.; et al. Adaptive finite-time bipartite consensus tracking control for heterogeneous nonlinear MASs with time-varying output constraints. *IEEE Trans. Autom. Sci. Eng.* **2023**, *21*, 6229–6238.
15. Zou, W.; Shi, P.; Xiang, Z.; et al. Finite-time consensus of second-order switched nonlinear multi-agent systems. *IEEE Trans. Neural Netw. Learn. Syst.* **2019**, *31*, 1757–1762.

16. Lei, J.; Li, Y.X.; Ahn, C.K. Optimizing multi-agent systems with uncertain dynamics: A finite-time adaptive distributed approach. *IEEE Trans. Signal Inf. Process. Over Netw.* **2023**, *9*, 865–874.
17. Fotiadis, F.; Rovithakis, G.A. Input-Constrained Prescribed Performance Control for High-Order MIMO Uncertain Nonlinear Systems via Reference Modification. *IEEE Trans. Autom. Control* **2023**, *69*, 3301–3308.
18. Li, Z.; Wang, X.; Guo, H.; et al. Distributed output feedback prescribed performance control for high-order nonlinear multi-agent systems. *IEEE Trans. Autom. Sci. Eng.* **2025**, *22*, 12730–12740.
19. Sui, S.; Chen, C.P.; Tong, S. Finite-time adaptive fuzzy prescribed performance control for high-order stochastic nonlinear systems. *IEEE Trans. Fuzzy Syst.* **2021**, *30*, 2227–2240.
20. Wang, H.; Bai, W.; Zhao, X.; et al. Finite-time-prescribed performance-based adaptive fuzzy control for strict-feedback nonlinear systems with dynamic uncertainty and actuator faults. *IEEE Trans. Cybern.* **2021**, *52*, 6959–6971.
21. Fang, L.; Ma, L.; Ding, S.; et al. Finite-time stabilization of high-order stochastic nonlinear systems with asymmetric output constraints. *IEEE Trans. Syst. Man Cybern. Syst.* **2020**, *51*, 7201–7213.
22. Xi, R.; Zhang, H.; Mu, Y.; et al. Finite-Time Control for High-Order Random Nonlinear Systems With Unknown Control Coefficients. *IEEE Trans. Autom. Sci. Eng.* **2024**, *22* 3172–3181.
23. Jiang, M.M.; Xie, X.J.; Zhang, K. Finite-time stabilization of stochastic high-order nonlinear systems with FT-SISS inverse dynamics. *IEEE Trans. Autom. Control* **2018**, *64*, 313–320.
24. Zhu, Y.; Niu, B.; Shang, Z.; et al. Distributed adaptive asymptotic consensus tracking control for stochastic nonlinear MASs with unknown control gains and output constraints. *IEEE Trans. Autom. Sci. Eng.* **2024**, *22*, 328–338.
25. Long, J.; Wang, W.; Huang, J.; et al. Adaptive leaderless consensus for uncertain high-order nonlinear multiagent systems with event-triggered communication. *IEEE Trans.Syst. Man Cybern. Syst.* **2022**, *52*, 7101–7111.
26. Deng, C.; Wen, C.; Wang, W.; et al. Distributed adaptive tracking control for high-order nonlinear multiagent systems over event-triggered communication. *IEEE Trans. Autom. Control* **2022**, *68*, 1176–1183.
27. Xing, L.; Wen, C.; Liu, Z.; et al. Event-Triggered Adaptive Control for a Class of Uncertain Nonlinear Systems. *IEEE Trans. Autom. Control* **2017**, *62*, 2071–2076.
28. Xing, L.; Wen, C.; Liu, Z.; et al. Adaptive compensation for actuator failures with event-triggered input. *Automatica* **2017**, *85*, 129–136.
29. Zhang, C.H.; Yang, G.H. Event-triggered adaptive output feedback control for a class of uncertain nonlinear systems with actuator failures. *IEEE Trans. Cybernetics* **2018**, *50*, 201–210.
30. Sun, Z.Y.; Zhou, C.; Liu, Z.G.; et al. Fast finite-time adaptive event-triggered tracking for uncertain nonlinear systems. *Int. J. Robust Nonlinear Control* **2020**, *30*, 7806–7821.
31. Wang, W.; Long, J.; Zhou, J.; et al. Adaptive backstepping based consensus tracking of uncertain nonlinear systems with event-triggered communication. *Automatica* **2021**, *133*, 109841.
32. Lin, W.; Qian, C. Adaptive control of nonlinearly parameterized systems: a nonsmooth feedback framework. *IEEE Trans. Autom. Control* **2002**, *47*, 757–774.
33. Qian, C.; Lin, W. Non-Lipschitz continuous stabilizers for nonlinear systems with uncontrollable unstable linearization. *Syst. Control. Letters* **2001**, *42*, 185–200.
34. Qian, C.; Lin, W. A continuous feedback approach to global strong stabilization of nonlinear systems. *IEEE Trans. Autom. Control* **2001**, *46*, 1061–1079.
35. Sun, Z.Y.; Zhou, C.; Liu, Z.G.; et al. Fast finite-time adaptive event-triggered tracking for uncertain nonlinear systems. *Int. J. Robust Nonlinear Control* **2020**, *30*, 7806–7821.
36. Chen, B.; Lin, C. Finite-Time Stabilization-Based Adaptive Fuzzy Control Design. *IEEE Trans. Fuzzy Syst.* **2021**, *29*, 2438–2443.
37. Liu, Y.; Liu, X.; Jing, Y.; et al. A novel finite-time adaptive fuzzy tracking control scheme for nonstrict feedback systems. *IEEE Trans. Fuzzy Syst.* **2018**, *27*, 646–658.
38. Qiu, J.; Wang, T.; Sun, K.; et al. Disturbance observer-based adaptive fuzzy control for strict-feedback nonlinear systems with finite-time prescribed performance. *IEEE Trans. Fuzzy Syst.* **2021**, *30*, 1175–1184.
39. Zhang, H.; Lewis, F.L. Adaptive cooperative tracking control of higher-order nonlinear systems with unknown dynamics. *Automatica* **2012**, *48*, 1432–1439.
40. Khoo, S.; Xie, L.; Man, Z. Robust finite-time consensus tracking algorithm for multirobot systems. *IEEE/ASME Trans. Mechatron.* **2009**, *14*, 219–228.